

Biochemical, Functional, and Pharmacological Characterization of AT-56, an Orally Active and Selective Inhibitor of Lipocalin-type Prostaglandin D Synthase*

Received for publication, November 12, 2008, and in revised form, January 5, 2009. Published, JBC Papers in Press, January 8, 2009, DOI 10.1074/jbc.M808593200

Daisuke Irikura^{†1,2}, Kosuke Aritake^{†1}, Nanae Nagata[‡], Toshihiko Maruyama[‡], Shigeru Shimamoto[§], and Yoshihiro Urade^{‡3}

From the [†]Department of Molecular Behavioral Biology, Osaka Bioscience Institute, 6-2-4 Furuedai, Suita, Osaka 565-0874, Japan and the [§]Graduate School of Pharmaceutical Sciences, Osaka University, 1-6 Yamadaoka, Suita, Osaka 565-0871, Japan

We report here that 4-dibenzo[*a,d*]cyclohepten-5-ylidene-1-[4-(2*H*-tetrazol-5-yl)-butyl]-piperidine (AT-56) is an orally active and selective inhibitor of lipocalin-type prostaglandin (PG) D synthase (L-PGDS). AT-56 inhibited human and mouse L-PGDSs in a concentration (3–250 μM)-dependent manner but did not affect the activities of hematopoietic PGD synthase (H-PGDS), cyclooxygenase-1 and -2, and microsomal PGE synthase-1. AT-56 inhibited the L-PGDS activity in a competitive manner against the substrate PGH₂ ($K_m = 14 \mu\text{M}$) with a K_i value of 75 μM but did not inhibit the binding of 13-*cis*-retinoic acid, a nonsubstrate lipophilic ligand, to L-PGDS. NMR titration analysis revealed that AT-56 occupied the catalytic pocket, but not the retinoid-binding pocket, of L-PGDS. AT-56 inhibited the production of PGD₂ by L-PGDS-expressing human TE-671 cells after stimulation with Ca²⁺ ionophore (5 μM A23187) with an IC₅₀ value of about 3 μM without affecting their production of PGE₂ and PGF_{2 α} but had no effect on the PGD₂ production by H-PGDS-expressing human megakaryocytes. Orally administered AT-56 (<30 mg/kg body weight) decreased the PGD₂ production to 40% in the brain of H-PGDS-deficient mice after a stab wound injury in a dose-dependent manner without affecting the production of PGE₂ and PGF_{2 α} and also suppressed the accumulation of eosinophils and monocytes in the broncho-alveolar lavage fluid from the antigen-induced lung inflammation model of human L-PGDS-transgenic mice.

PGD₂⁴ is a lipid mediator involved in sleep (1, 2) and inflammatory responses (3). PGD₂ activates two different types of

receptors (*i.e.* DP₁ (4) and DP₂ (also known as CRTH2 (5))). PGD₂ regulates sleep (2, 6) and pain (7) via DP₁ receptors in the central nervous system. This prostanoid also causes contraction of airway smooth muscle via DP₁ receptors (8) and mediates chemotaxis of eosinophils and basophils into the lung via DP₂ receptors (9) in the periphery. Therefore, PGD₂ coordinately regulates allergic reactions, especially airway inflammation, via these two receptors (9).

PGD₂ is formed by the following sequence of enzyme reactions after cell activation: 1) cytosolic phospholipase A₂ is translocated to the endoplasmic reticulum and perinuclear membranes in a Ca²⁺-dependent manner, where it cleaves arachidonic acid from the membrane phospholipids; 2) arachidonic acid is converted to PGH₂, a common precursor of various prostanoids, by the membrane-bound cyclooxygenases (COXs); and 3) PGH₂ is further isomerized to PGD₂ by PGD synthase (PGDS). There are two distinct types of PGDS, namely lipocalin-type PGDS (L-PGDS) (10–13) and hematopoietic PGDS (H-PGDS) (14–16).

L-PGDS contributes to the production of PGD₂ in the central nervous system (10, 17, 18), ocular tissues (19), cardiovascular systems (20), and male genital organs (21) of various mammals and is involved in the regulation of non-rapid eye movement sleep (2, 22), sex determination (23), protection of atherosclerosis (24, 25), and adipogenesis (26). L-PGDS is secreted into the cerebrospinal fluid (CSF) (27, 28), seminal plasma (29, 30), and plasma (20) as β -trace, a major protein in human CSF (31).

L-PGDS is the only enzyme among the members of the lipocalin gene family (11), which is composed of various secretory proteins involved in binding and transporting small lipophilic substances, such as retinoids and thyroids (32). L-PGDS also binds retinoic acid, retinal (33), biliverdin (34), bilirubin (34), gangliosides (35), and amyloid β peptides (36) with high affinities of $K_d = 20$ –200 nM, indicating that L-PGDS may act as a transporter protein of these lipophilic compounds and as an endogenous chaperon to prevent amyloid β aggregation. On the other hand, H-PGDS is the first known vertebrate homolog of the σ class of glutathione *S*-transferases (37). Because both of these enzymes have evolved from different origins to acquire the same catalytic function, these two enzymes are considered to be a new example of functional convergence (38, 39).

Inorganic quadrivalent selenium (Se⁴⁺) compounds are known to be noncompetitive and reversible inhibitors of

* This work was supported in part by a grant from the Japan Foundation for Applied Enzymology (to K. A.), Grant-in Aid for Scientific Research of MEXT 19590094 (to K. A.), and Osaka City. The costs of publication of this article were defrayed in part by the payment of page charges. This article must therefore be hereby marked "advertisement" in accordance with 18 U.S.C. Section 1734 solely to indicate this fact.

Author's Choice—Final version full access.

¹ Both of these authors contributed equally to this work.

² Present address: Nippon Bio-test Laboratories Inc., 1-15-3 Higashitokura, Kokubunji, Tokyo 185-0002, Japan.

³ To whom correspondence should be addressed. Tel.: 81-6-6872-4851; Fax: 81-6-6872-2841; E-mail: uradey@obi.or.jp.

⁴ The abbreviations and trivial names used are: PGD₂, PGE₂, PGF_{2 α} , and PGH₂, prostaglandin D₂, E₂, F_{2 α} , and H₂, respectively; PG, prostaglandin; AT-56, 4-dibenzo[*a,d*]cyclohepten-5-ylidene-1-[4-(2*H*-tetrazol-5-yl)-butyl]-piperidine; PGDS, prostaglandin D synthase; L-PGDS, lipocalin-type prostaglandin D synthase; H-PGDS, hematopoietic prostaglandin D synthase; CSF, cerebrospinal fluid; COX, cyclooxygenase; KO, knockout; TG, transgenic; HQL-79, 4-benzhydryloxy-1-(3-(1*H*-tetrazol-5-yl)-propyl)-piperidine.

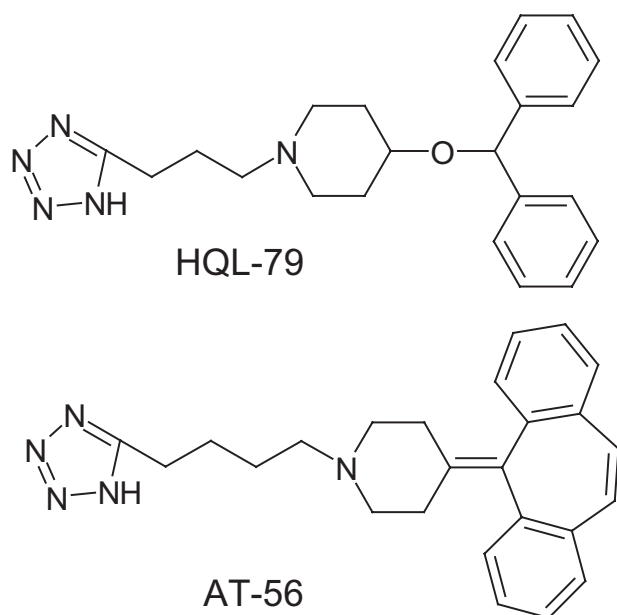


FIGURE 1. Chemical structures of HQL-79 and AT-56.

L-PGDS (40) and to inhibit the sleep of animals in a time- and dose-dependent manner after infusion into the third ventricle of rats or an intraperitoneal injection into mice (2, 41). However, no organic inhibitor of L-PGDS has been reported until now. We recently found that 4-benzhydryloxy-1-(3-(1*H*-tetrazol-5-yl)-propyl)-piperidine (HQL-79; Fig. 1) is an orally active and selective inhibitor of H-PGDS (42). Because L-PGDS catalyzes the same reaction as H-PGDS, we suspected that some derivative(s) of HQL-79 might have an inhibition activity toward L-PGDS. Among various tetrazol compounds, we found that 4-dibenzo[*a,d*]cyclohepten-5-ylidene-1-[4-(2*H*-tetrazol-5-yl)-butyl]-piperidine (AT-56; Fig. 1) is a specific inhibitor of L-PGDS (43), having a higher potency and biological availability than seleno-compounds *in vivo*.

In the present study, we characterized AT-56 and found it to be a competitive inhibitor of L-PGDS against PGH₂ by kinetic analysis and also used NMR analysis to determine the binding mode of AT-56 to L-PGDS. In addition we found that AT-56 inhibited the production of PGD₂ by L-PGDS-expressing cultured cells, H-PGDS gene knock-out (KO) mice, and human L-PGDS overexpressing transgenic (TG) mice.

EXPERIMENTAL PROCEDURES

Chemicals—AT-56 was a generous gift from TAIHO Pharmaceutical Company (Saitama, Japan). AT-56 was dissolved in DMSO for *in vitro* experiments and in 0.5% methylcellulose for oral administration to mice, due to its high lipophilicity. In aqueous solution, the maximum solubility of AT-56 was determined to be 90 μM in saline containing 1% DMSO and 260 μM in 10% DMSO, as determined by UV absorption at 287 nm. Other reagents were purchased from Sigma or Wako (Osaka, Japan), unless otherwise specified.

Purification of Human CSF L-PGDS (β-Trace) and Recombinant Mouse L-PGDS—Human CSF L-PGDS (β-trace) was purified from human CSF, which was donated by Dr. M. Mase (Nagoya City University Hospital), as reported (36).

The full-length cDNA for mouse L-PGDS, which is composed of 189 amino acid residues (GenBankTM accession number X89222), was ligated into the BamHI-EcoRI site of the expression vector pGEX-2T plasmid (GE Healthcare). The N-terminal 22-amino acid residues of the signal peptide were deleted, and the C89A/C186A- and W54A-substituted recombinant enzymes were expressed in *Escherichia coli* DH5α (TOYOBO, Osaka, Japan). Site-directed mutagenesis was performed by using a QuikChange[®] site-directed mutagenesis kit (Stratagene, La Jolla, CA). The recombinant enzymes retained PGDS activity comparable with that of the wild-type enzyme and were stable for long term use. The mutated L-PGDS was expressed as a GSH transferase fusion protein, purified by column chromatography with GSH-Sepharose 4B (GE Healthcare), and eluted from the column by incubation with thrombin (100 units/100 μl of resin), as reported previously (44). The recombinant protein was further purified to apparent homogeneity by gel filtration chromatography with Superdex 75 in 5 mM Tris/HCl (pH 8.0).

Fluorescence Quenching Assays—13-*cis*-Retinoic acid and AT-56 were dissolved in DMSO to give a 2 mM stock solution. Various concentrations of 13-*cis*-retinoic acid and AT-56 in 10 μl of DMSO were added to the L-PGDS solution in 990 μl of 5 mM Tris/HCl (pH 8.0). After incubation at room temperature for 60 min, the intrinsic tryptophan fluorescence was detected with an FP-750 spectrofluorometer (JASCO, Tokyo, Japan) at an excitation wavelength at 282 nm and an emission wavelength at 338 nm, as reported previously (44).

Enzyme Activity Assays—Enzyme activities of L-PGDS (45), H-PGDS (46), and microsomal PGE synthase (m-PGES-1 (47)) were measured with 10 μM [1-¹⁴C]PGH₂ as a substrate in 100 mM Tris-HCl, pH 8.0, in the presence of 1 mM GSH, 0.1 mg/ml IgG, and 10% DMSO. The activities of COX-1 and COX-2 were measured as described earlier (48) with 50 μM [1-¹⁴C]arachidonic acid (PerkinElmer) used as a substrate in 100 mM Tris-HCl, pH 8.0, containing 2 μM hemein, 5 mM L-tryptophan, 0.1 mg/ml IgG, and 10% DMSO. The products were separated by thin layer chromatography. The conversion rate from ¹⁴C-labeled substrate to ¹⁴C-labeled products was calculated by using an imaging plate system (Fuji Film, Tokyo, Japan). The kinetic constants were determined by Lineweaver-Burk plots prepared with SigmaPlot software (version 10.0 for Windows; Systat Software, Inc.).

NMR Titration Experiment—The NMR samples of mouse L-PGDS were prepared in a mixture of 50 mM sodium phosphate in 75% H₂O, 15% D₂O, 10% DMSO at pH 7.0, as reported previously (49). The protein concentration was adjusted to ~1 mM in a 5-mm microcell NMR tube (Shigemi, Tokyo, Japan) for NMR experiments. NMR experiments were performed at 27.5 °C by using an INOVA600 spectrometer (Varian, Palo Alto, CA) equipped with shielded gradient triple resonance probes (49).

The binding of L-PGDS to AT-56 was monitored by NMR titration of ¹⁵N-labeled L-PGDS with unlabeled ligands by using ¹H-¹⁵N heteronuclear single quantum correlation experiments. The combined ¹H and ¹⁵N chemical shift changes over the range of the titration from 0 to 2.0 equivalents of AT-56 were plotted. The composite chemical shift differences were calcu-

lated according to the empirical equation $\Delta\delta_{\text{tot}} = \{(\Delta\delta_{\text{HN}} \times W_{\text{HN}})^2 + (\Delta\delta_{\text{N}} \times W_{\text{N}})^2\}^{1/2}$, where $\Delta\delta_{\text{HN}}$ and $\Delta\delta_{\text{N}}$ are the chemical shift changes of ^1H and ^{15}N , respectively. The weighting factors used were $W_{\text{HN}} = 1$ and $W_{\text{N}} = 0.2$.

PG Production by Cultured Cells—L-PGDS-expressing human medulloblastoma TE-671 cells and H-PGDS-possessing human megakaryoblastic MEG-01S cells were purchased from American Type Culture Collection. TE-671 (1×10^6 cells/well) and MEG-01S (5×10^5 /well) cells were seeded into multiplates and cultured in Dulbecco's modified Eagle's medium supplemented with 10% heat-inactivated fetal bovine serum, 4 mM L-glutamine, 4.5 g/liter glucose, 100 units/ml penicillin, and 100 $\mu\text{g}/\text{ml}$ streptomycin sulfate under a 5% CO_2 atmosphere at 37 °C. MEG-01S cells were caused to differentiate by treatment with 12-*O*-tetradecanoylphorbol-13-acetate to express H-PGDS and COX-1, as described previously (50).

After the cells had been cultured for 1 day, AT-56 was added to them at different doses ranging from 0 to 100 μM , and the cells were then incubated at 37 °C for 10 min. Thereafter, they were stimulated with a calcium ionophore, A23187 (5 μM), at 37 °C for 15 min. The culture media were harvested and centrifuged at $10,000 \times g$ for 5 min to remove the cells, and the supernatant was removed and stored at -80 °C until the measurements of PGs could be made. In some experiments, these cells were prelabeled with [$1\text{-}^{14}\text{C}$]arachidonic acid (3.7 kBq/well) for 12 h before the assay. PGD_2 , PGE_2 , and $\text{PGF}_{2\alpha}$ in the culture medium were quantified as described below.

PG Production by Stab Wound Brain Injury—The protocols used for all animal experiments in this study were approved by the Animal Research Committee of the Osaka Bioscience Institute.

H-PGDS KO mice (14–16-week-old males or females weighing 25–30 g, C57BL/6 strain) (2, 51) containing only L-PGDS were used for the stab injury model of the brain. AT-56 of various doses (1, 3, 10, and 30 mg/kg body weight) was administered orally to H-PGDS KO mice 1 h before the stab wound injury. Under pentobarbital (50 mg/kg) anesthesia, a 25-gauge needle was inserted into the frontal cortex of the brain of H-PGDS KO mice at a position 2 mm caudal to the bregma, 2 mm lateral to the sagittal suture, and 1 mm deep. After the needle had been withdrawn, the brains were harvested, immediately frozen in liquid nitrogen, and stored in a deep freezer (-80 °C) until the measurements of PG contents could be made.

Measurement of PG Contents—The amounts of PGs in the cell culture media and brain tissues were determined as described previously (22). In brief, the cell culture media and the frozen brain tissues were homogenized in ethanol containing 0.02% HCl at pH 2.0 and [^3H]PGD₂, [^3H]PGE₂, and [^3H]PGF_{2 α} (PerkinElmer Life Sciences) as tracers to estimate the recovery during the purification procedure. After centrifugation at $500 \times g$ for 20 min, the ethanol extracts were applied onto Sep-Pak C18 cartridges (Waters Associates, Milford, MA), washed with hexane, eluted with ethyl acetate, and fractionated by reverse-phase high performance liquid chromatography. The amounts of PGD_2 , PGE_2 , and $\text{PGF}_{2\alpha}$ were measured by using their respective enzyme immunoassay kits (Cayman

Chemical, Ann Arbor, MI), according to the manufacturer's instructions.

L-PGDS-mediated Allergic Airway Inflammation—Human L-PGDS-overexpressing TG mice (14–16-week-old males weighing 25–30 g, FVB strain (22)) were actively sensitized by an intraperitoneal injection of 10 μg of ovalbumin (Sigma) in 0.2 ml of aluminum hydroxide gel (Serva, Heidelberg, Germany) on days 0 and 14 and then exposed to aerosolized ovalbumin (50 mg/ml in sterile saline) for 20 min on day 21 (52). At 2 days after the ovalbumin challenge, the bronchoalveolar lavage fluid was collected as reported previously (52). Total and differential cell counts (500 cells) were obtained based on standard morphologic criteria after the cells had been cytospun onto glass slides and stained with Diff-Quik (Dade Diagnostics).

Pharmacokinetics of AT-56—Male C57BL/6 mice (7 weeks old, weighing 22–26 g; Japan SLC, Shizuoka, Japan) were given a single oral dose of 10 mg/kg AT-56 or a single intravenous dose of 2 mg/kg AT-56. Plasma was collected after euthanasia from 3 mice/group at 30 min and 1, 2, 4, 8, and 24 h for oral administration and 5 and 30 min and 1, 2, 4, 8, 12, and 24 h after intravenous dosing. Whole blood sample was collected into a heparinized syringe at each time point. Plasma was obtained by centrifugation and was stored at -30 °C until analysis.

Concentrations of AT-56 in plasma were determined by high performance liquid chromatography coupled to mass spectrometry. Samples were separated by chromatography with a Cadenza HS-C18 column (2 mm \times 150 mm; Imtakt Corp., Kyoto, Japan) at a column temperature of 33 °C with a 5–90% acetonitrile gradient in 0.02% formic acid at a flow rate of 0.2 ml/min for 12 min. Injection volume was 10 μl . AT-56 was detected by mass spectrometry with the system (Waters Associates) composed of the 2695 separation module, 996 photodiode array detector, and ZQ-4000 mass spectrometry detector with an electrospray ionization source. The electrospray ionization interface was operated at a source temperature of 115 °C and a desolvation temperature of 350 °C. Cone gas and desolvation gas flow were 124 and 606 liters/h, respectively. Cone voltage for AT-56 was positive 33 V for $m/z = 398$. Pharmacokinetic parameters were calculated using noncompartmental analysis with WinNonlin, version 5.0.1 (Pharsight, Mountain View, CA).

Statistics—Comparisons were analyzed for statistical significance by Dunnett's multicomparison test using SigmaPlot (Systat Software, CA). $p < 0.05$ was considered significant.

RESULTS

Inhibition of the L-PGDS Activity by AT-56—AT-56 inhibited the PGDS activity of both β -trace purified from human CSF and purified recombinant mouse L-PGDS C89A/C186A mutant in a concentration (10–250 μM)-dependent manner. The L-PGDS activity of both preparations was inhibited to 30% with 250 μM AT-56, and the IC_{50} value was calculated to be 95 μM . However, the activities of the purified COX-1, COX-2, m-PGES-1, or H-PGDS in the arachidonate cascade were not significantly affected by AT-56 up to 250 μM (Fig. 2A).

Kinetic experiments revealed that AT-56 inhibited the recombinant L-PGDS in a competitive manner against the substrate PGH₂, as shown in Lineweaver-Burk plots (Fig. 2B), in

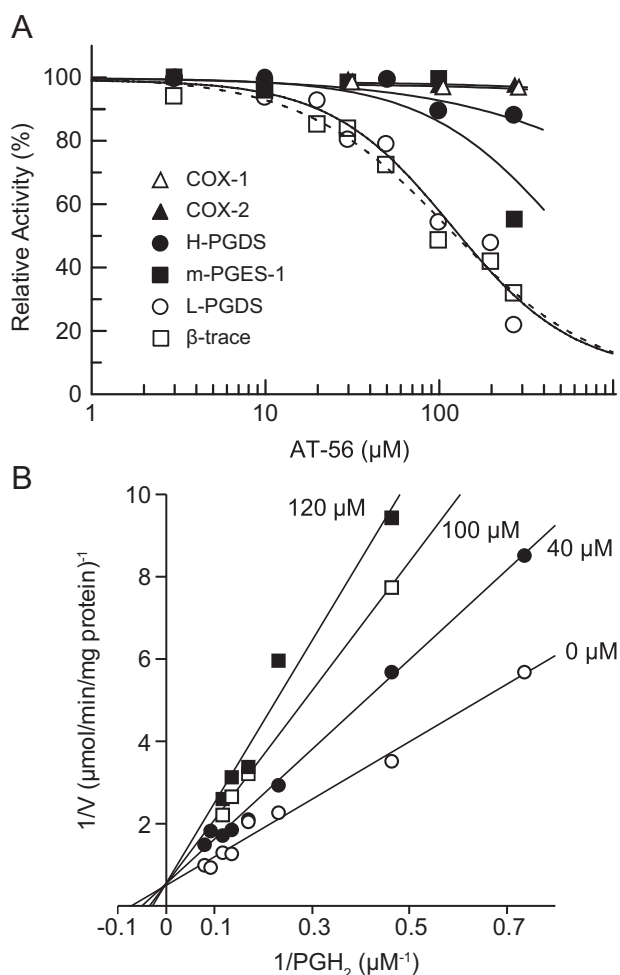


FIGURE 2. **Specific inhibition of L-PGDS by AT-56.** A, human CSF L-PGDS (β -trace), the recombinant mouse L-PGDS C89A/C186A mutant, the purified m-PGES-1, and H-PGDS were incubated with $10 \mu\text{M}$ PGH_2 and 1 mM GSH at 25°C for 30 s in the presence of 0 – $250 \mu\text{M}$ AT-56 in 10% DMSO. The purified COX-1 and COX-2 were incubated with $50 \mu\text{M}$ arachidonic acid in the presence of 0 – $250 \mu\text{M}$ AT-56. B, Lineweaver-Burk plot for L-PGDS. Recombinant mouse L-PGDS C89A/C186A mutant was incubated with various concentrations of PGH_2 (3 – $20 \mu\text{M}$), 100 mM Tris-HCl (pH 8), and 1 mM dithiothreitol in the presence of 0 (\circ), 40 (\bullet), 100 (\square), or $120 \mu\text{M}$ (\blacksquare) AT-56 in 10% DMSO.

which the V_{max} value remained unchanged but the K_m value increased when the AT-56 concentration was increased (0 – $120 \mu\text{M}$). The apparent K_i value of AT-56 was calculated to be $75 \mu\text{M}$, which was 5.3 -fold higher than the K_m value of the L-PGDS activity for PGH_2 ($14 \mu\text{M}$) in the presence of 10% DMSO.

Binding Interaction between L-PGDS and AT-56 Analyzed by NMR—We have previously determined the NMR structure of the mouse L-PGDS C89A/C186A mutant (49). The interaction sites of L-PGDS with AT-56 were determined by the chemical shift perturbation method (53) based on the two-dimensional ^1H - ^{15}N heteronuclear single quantum correlation NMR spectra of L-PGDS after the successive addition of AT-56 (Fig. 3). Upon AT-56 binding, large changes ($>0.08 \text{ ppm}$) of chemical shift were observed at several amino acid residues of L-PGDS (*i.e.* Ser⁵², Thr⁸⁰, Met⁹⁴, and His¹¹⁶) (Fig. 3A). These residues are located at the upper part of the central cavity of the β -barrel structure of the L-PGDS molecule (Protein Data Bank code 2E4J; Fig. 3B), in which the PGH_2 -binding site containing the catalytic center of Cys⁶⁵ is located (49). However, the AT-56

binding did not cause any significant chemical shift in the regions of the retinoic acid-binding pocket at the lower part of the central cavity of L-PGDS (49).

Fluorescence Quenching Study on L-PGDS after Binding of AT-56—To confirm the mode of binding of AT-56 to L-PGDS, we examined the fluorescence quenching of intrinsic Trp residues of mouse L-PGDS after incubation with AT-56. Mouse L-PGDS contains two tryptophan residues, at positions 43 and 54, the former of which is located at the bottom of barrel and the latter in the AB-loop at the entrance of the central cavity of L-PGDS (49). The C89A/C186A mutant of mouse L-PGDS showed fluorescence quenching by the addition of AT-56 (Fig. 4A) in a concentration-dependent manner, and the fluorescence intensity was decreased to about 60% in the presence of $10 \mu\text{M}$ AT-56. On the other hand, the W54A/C89A/C186A mutant showed about 60% of the tryptophan fluorescence of the C89A/C186A mutant in the absence of AT-56 and did not show the fluorescence quenching in the presence of $10 \mu\text{M}$ AT-56 (Fig. 4A). The C89A/C186A mutant showed fluorescence quenching by the addition of *13-cis*-retinoic acid in a concentration-dependent manner, with the fluorescence intensity being decreased to about 8% in the presence of $10 \mu\text{M}$ *13-cis*-retinoic acid (Fig. 4B). The C89A/C186A mutant in the presence of $10 \mu\text{M}$ AT-56 and the W54A/C89A/C186A mutant showed about 60% of the fluorescence intensity of the C89A/C186A mutant in the absence of $10 \mu\text{M}$ AT-56. In both cases, the fluorescence intensity was decreased by the addition of *13-cis*-retinoic acid in a concentration-dependent manner to $<10\%$ in the presence of $10 \mu\text{M}$ *13-cis*-retinoic acid, giving the same fluorescence quenching curves even in the presence of $10 \mu\text{M}$ AT-56. These results indicate that AT-56 binds near Trp⁵⁴ in the AB-loop of L-PGDS but not to the Trp⁴³ residue in the retinoid-binding pocket, being consistent with the results obtained by NMR titration analysis.

Inhibition of PGD_2 Production in L-PGDS-expressing Human Medulloblastoma TE-671 Cells by AT-56—Human medulloblastoma TE-671 cells constitutively express L-PGDS (54). We pretreated TE-671 cells for 10 min with 0 to $30 \mu\text{M}$ AT-56, stimulated them with calcium ionophore A23187 ($5 \mu\text{M}$) at 37°C for 15 min , and then determined the production of PGD_2 , PGE_2 , and $\text{PGF}_{2\alpha}$ by enzyme immunoassay to investigate the effects of AT-56 on PG production by these cells. AT-56 dose-dependently inhibited the production of PGD_2 without affecting the production of PGE_2 and $\text{PGF}_{2\alpha}$ (Fig. 5A).

Dose-dependent inhibition of the A23187-induced PGD_2 production by AT-56 (3 – $100 \mu\text{M}$) was also confirmed by using [1 - ^{14}C]arachidonic acid-prelabeled TE-671 cells (Fig. 5B). However, the production of other ^{14}C -labeled metabolites was not inhibited by AT-56 up to $100 \mu\text{M}$. Moreover, AT-56 had no effect on the production of PGD_2 by human H-PGDS-expressing MEG-01S cells (50). H-PGDS-specific inhibitor, HQL-79, inhibited PGD_2 production from MEG-01S cells but not from TE-671 cells. These results indicate that AT-56 selectively inhibits PGD_2 production catalyzed by L-PGDS without affecting the production of other prostanoids.

Suppression of PGD_2 Production in the Stab-wounded Brain by Oral Administration of AT-56—To investigate the effect of AT-56 *in vivo*, we used H-PGDS KO mice, which express only

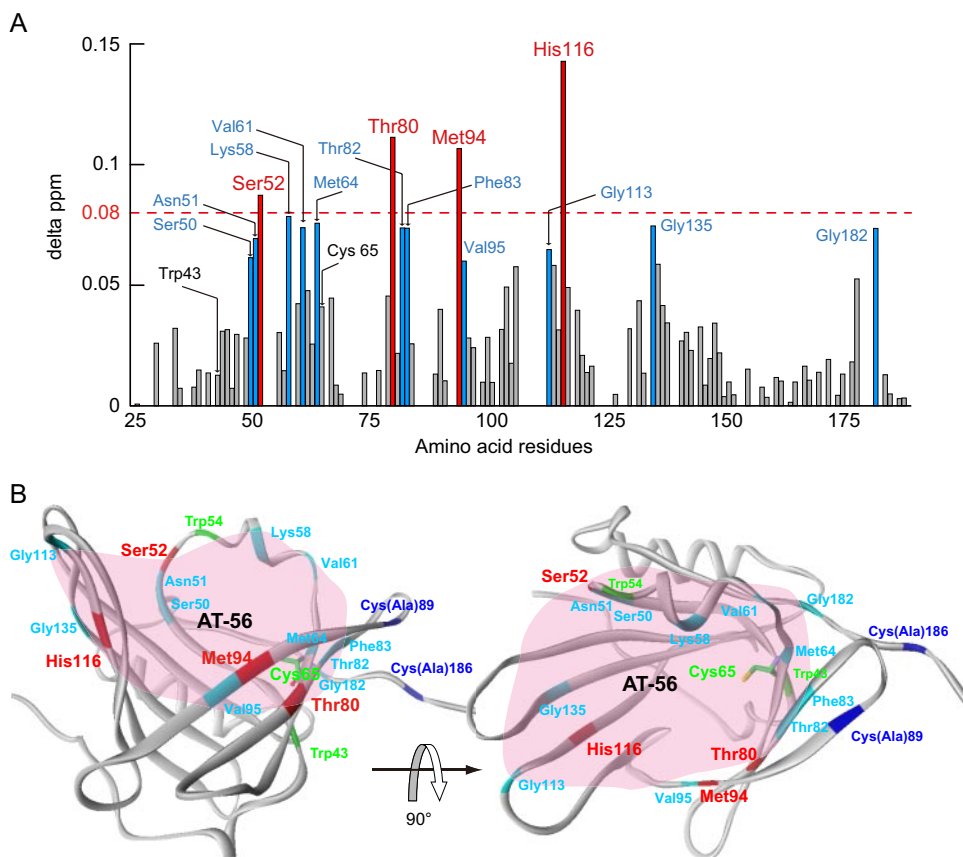


FIGURE 3. **Interactions of L-PGDS with AT-56 as examined by NMR.** A, composite ^1H and ^{15}N chemical shift differences (Δ ppm) versus the amino acid sequence of recombinant mouse L-PGDS C89A/C186A mutant. B, overall structure of L-PGDS after AT-56 binding in a ribbon representation. In both panels, the residues with relatively large changes in chemical shift (≥ 0.08) are represented in red, whereas residues with shifts in the middle range ($0.06 \leq \Delta \text{ppm} < 0.08$) are shown in sky blue. In B, the AT-56-binding site predicted from NMR signal perturbation is shaded in pink.

L-PGDS in all of their organs (51). In a stab wound brain injury model, the PGD_2 content in the brain of the wounded H-PGDS KO mice (118 ± 22 ng/brain) was significantly increased as compared with that of the control mice without injury (0.23 ± 0.04 ng/brain). When various doses of AT-56 were administered orally 1 h before the injury, the total amount of PGD_2 in the brain decreased dose-dependently to 40% with 30 mg/kg AT-56 (Fig. 6A). The amounts of PGE_2 and $\text{PGF}_{2\alpha}$ in the brain were not significantly changed in any conditions (Fig. 6A). These results indicate that orally administered AT-56 inhibited the L-PGDS reaction in the brain.

Suppression of L-PGDS-mediated Allergic Airway Inflammation by AT-56—We next evaluated the therapeutic effect of AT-56 on PGD_2 -mediated lung inflammation. Human L-PGDS TG mice were used in an OVA-induced lung inflammation model (52). The numbers of total cells and infiltrating eosinophils and monocytes in the bronchoalveolar lavage fluid of the L-PGDS TG mice were dose-dependently decreased to 75, 50, and 96% (actual numbers: 8.7 ± 1.9 , 2.53 ± 0.73 , and $6.16 \pm 1.14 \times 10^4$ cells/ml for total cells, eosinophils, and monocytes, respectively) in 1 mg/kg AT-56-treated mice and to 23, 6, and 41% (2.7 ± 0.4 , 0.31 ± 0.14 , and $2.59 \pm 0.3 \times 10^4$ cells/ml, respectively) in 10 mg/kg AT-56-treated ones compared with the numbers for the vehicle-administered mice (11.6 ± 1.6 ,

5.28 ± 1.37 , and $6.36 \pm 0.72 \times 10^4$ cells/ml, respectively) (Fig. 6B). These results demonstrate that AT-56 prevented the eosinophil infiltration by inhibiting transgenic human L-PGDS *in vivo*.

Pharmacokinetic Properties of AT-56—We also determined pharmacokinetic properties of AT-56. Fig. 7 shows the time courses of the plasma concentration of AT-56 after an oral administration to mice at a dose of 10 mg/kg and an intravenous bolus injection of 2 mg/kg. Table 1 summarizes pharmacokinetic parameters of AT-56. After the oral administration, the plasma level of AT-56 reached the maximum ($2.15 \mu\text{g/ml}$) within 30 min and decreased with time to be lower than the detection limit (0.4 ng/ml) at 12 h after the administration. The area under the concentration-time curve was calculated to be 2.18 and $8.95 \mu\text{g/ml} \times \text{h}$ after the intravenous administration of 2 mg/kg and the oral administration of 10 mg/kg, respectively. Based on these data, bioavailability of AT-56 was calculated to be 82%, indicating that orally administered AT-56 was well absorbed in mice.

DISCUSSION

In the present study, we demonstrated that AT-56 is an orally active inhibitor specific for L-PGDS with a high bioavailability. The results of the kinetic analyses indicated that AT-56 was a competitive inhibitor against the substrate, PGH_2 . NMR titration analysis revealed that AT-56 bound to the catalytic pocket of L-PGDS, in which the catalytic center Cys⁶⁵ is located (49), being consistent with the competitive inhibition of L-PGDS by AT-56. The NMR solution structure is also in good agreement with the results of the fluorescence quenching analysis of L-PGDS, in which AT-56 interacted with the upper part of L-PGDS containing Trp⁵⁴ but did not affect the fluorescence of Trp⁴³ located in the retinoic acid-binding pocket at the bottom of the hydrophobic cavity of the enzyme.

Our data demonstrate that AT-56 inhibited the isomerization reaction of PGH_2 to PGD_2 catalyzed by L-PGDS in a competitive manner against PGH_2 with a K_i value of $75 \mu\text{M}$ (Fig. 2), which was 5.3-fold higher than the K_m value of the L-PGDS activity for PGH_2 ($14 \mu\text{M}$) in the presence of 10% DMSO. Therefore, in the enzyme assay, AT-56 inhibited the enzyme activity clearly in a high concentration range in the presence of PGH_2 . On the other hand, in the absence of PGH_2 , AT-56 binds to the enzyme and induces the fluorescence quenching even in the low concentration range. Various inorganic selenium compounds are also known to inhibit both the purified L-PGDS and

L-PGDS Inhibitor AT-56

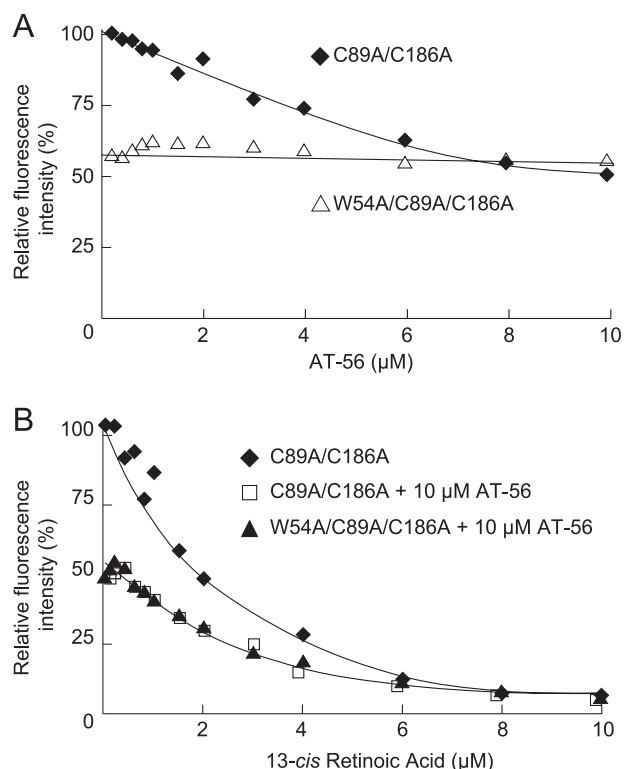


FIGURE 4. Tryptophan fluorescence quenching by AT-56. *A*, fluorescence quenching of intrinsic tryptophan of C89A/C186A mutant (◆) and W54A/C89A/C186A mutant (▲) of mouse L-PGDS by incubation with AT-56. *B*, fluorescence quenching of intrinsic tryptophan of the mouse L-PGDS C89A/C186A mutant in the absence (◆) or presence (□) of 10 μM AT-56 and that for the W54A/C89A/C186A mutant in the presence of 10 μM AT-56 (▲) by incubation with 13-*cis*-retinoic acid.

the enzyme in the crude brain supernatant in a noncompetitive manner with a K_i value of 10 μM (40). The K_i value of AT-56 was 7.5-fold higher than that of SeCl₄. However, the inhibition mode of AT-56 was quite different from that of selenium; *i.e.* this is the first competitive inhibitor of L-PGDS against PGH₂ to be reported. When the same dose of various seleno-compounds was used in cell cultures, such compounds reduced PGD₂ production; however, their efficacy cannot be attributed solely to the effects on the PGD₂ pathway. Seleno-compounds also inhibited the release of arachidonic acid and the production of all PGs due to the lack of specificity of action. In contrast, when human TE-671 cells were stimulated with the Ca²⁺ ionophore A23187 in the presence of 10 μM AT-56, only a base level of PGD₂ biosynthesis was observed without changing the arachidonic acid release (Fig. 5*B*).

At present, the reason why the IC₅₀ value in the cell was lower than the IC₅₀ and K_i values for purified L-PGDS is unknown. L-PGDS requires sulfhydryl compounds, such as reduced GSH, dithiothreitol, or β -mercaptoethanol, for its catalytic reaction, although it catalyzes the isomerization of the substrate PGH₂ to the product PGD₂. The endogenous sulfhydryl compounds have not been identified in its reaction, and GSH or dithiothreitol have been used as a reductant in *in vitro* experiments. In this present study, we used GSH for the enzyme inhibition assay of AT-56. Thus, it is possible that the reductant for the L-PGDS reaction is different from the endogenous one. It might be also possible that L-PGDS requires some other cofactor for its catal-

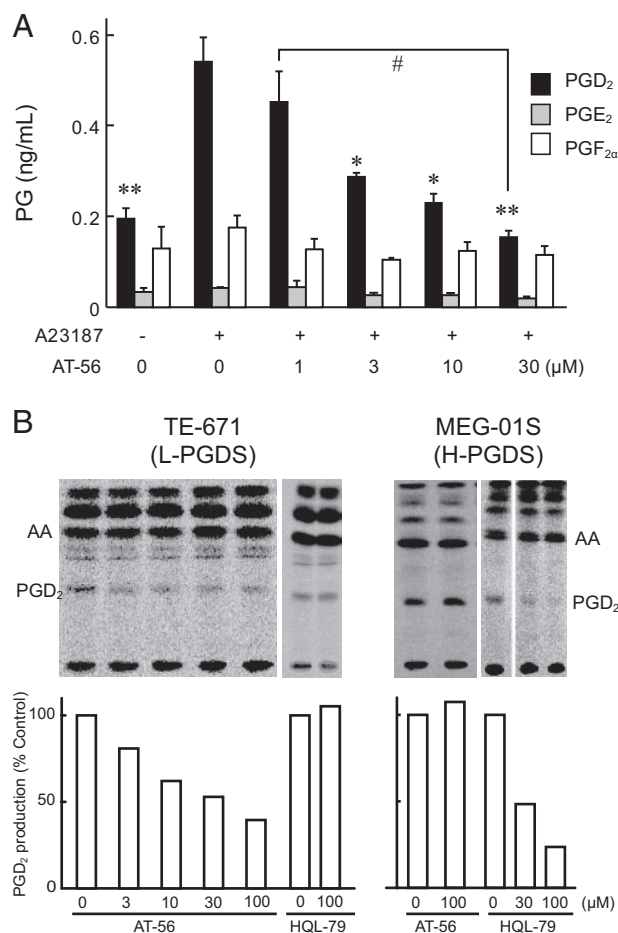


FIGURE 5. Inhibition of L-PGDS activity by AT-56 in TE-671 cells but not in MEG-015 cells. TE-671 cells expressing L-PGDS were pretreated with various concentrations of AT-56 for 15 min and then incubated with or without 5 μM A23187 for 10 min to measure prompt PGD₂ release. *A*, the amount of PGD₂ released from TE-671 cells was measured by enzyme immunoassay. AT-56 dose-dependently inhibits PGD₂ production from L-PGDS-expressing TE-671. Data are presented as the mean \pm S.E. *, $p < 0.05$; **, $p < 0.01$ as compared with the value in the absence of AT-56 and in the presence of A23187. #, $p < 0.05$ as compared with the value in the presence of 1 μM AT-56 (Dunnett's test). *B*, selective inhibition by AT-56 of [¹⁴C]PGD₂ production in TE-671 cells and in H-PGDS-expressing MEG-015 cells. TE-671 and MEG-015 cells were prelabeled with [¹⁴C]arachidonic acid and stimulated with 5 μM A23187 for 15 min in the presence of various concentrations of AT-56 (3–100 μM). Radio-labeled arachidonic acid and its metabolites were extracted from the culture medium, separated by thin layer chromatography, and analyzed by autoradiography. AA, arachidonic acid.

ysis. AT-56 might effectively inhibit the L-PGDS reaction in the presence of such endogenous cofactor.

Recently, we demonstrated that L-PGDS produced PGD₂ coupled with COX-2 in TE-671 cells (43). L-PGDS coupled to COX-2 may be more sensitive to AT-56 than L-PGDS itself. Since AT-56 is a relatively lipophilic compound, its local concentration around the L-PGDS-COX-2 complex within endoplasmic reticulum may be high enough to efficiently inhibit the production of PGD₂ within the cell.

Although both L-PGDS and H-PGDS became evolutionarily diversified from quite different ancestor gene families (38, 39), these enzymes can catalyze the same isomerization reaction. HQL-79 recently has been identified as an H-PGDS inhibitor. In this study, we found that AT-56, which is an HQL-79-derivative compound, also has an inhibitory activity against the

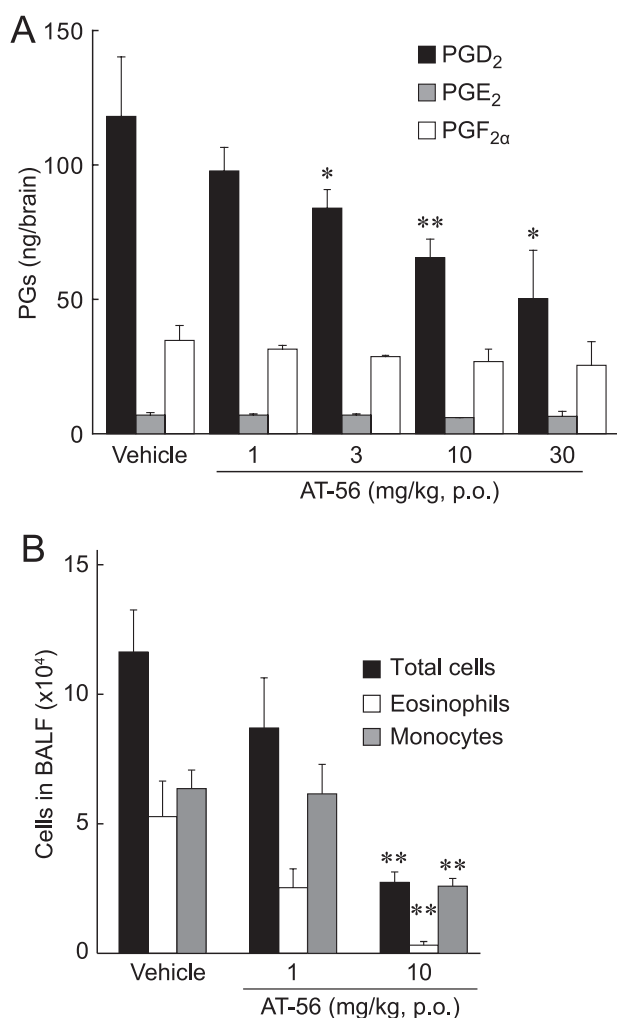


FIGURE 6. Inhibitory effect of AT-56 on PGD₂ production by stab wounding in H-PGDS KO mice and therapeutic effect on antigen-induced lung inflammation in human L-PGDS TG mice. A, AT-56 was orally administered 1 h before the stab wounding, and brains were collected 10 min after the wounding. B, AT-56 was orally administered 1 h before and 24 h after the antigen exposure. The accumulated cells in the bronchoalveolar lavage fluid were collected 48 h after the antigen exposure. Data are presented as the mean \pm S.E. *, $p < 0.05$; **, $p < 0.01$ as compared with the vehicle-treated group (Dunnett's test). *p.o.*, *per os*. BALF, bronchoalveolar lavage fluid.

L-PGDS reaction both *in vitro* and *in vivo*, suggesting that the active site architecture for the substrate binding and the catalytic reaction mechanism of L-PGDS could be similar to those of H-PGDS.

Here, we demonstrated pharmacologically and biochemically that AT-56 is an orally effective inhibitor selective for L-PGDS. Especially, it should be noted that AT-56 specifically inhibited the production of PGD₂ catalyzed by L-PGDS but only marginally affected the production of other prostanoids. In this sense, AT-56 is an even better PGD₂-blocking compound than inorganic selenium compounds. Earlier we demonstrated that PGD₂ produced by L-PGDS regulates physiological sleep (1) and pain (7) and also that L-PGDS acts as an extracellular transporter for various useful or harmful hydrophobic compounds (34–36). Thus, AT-56 may be predicted to selectively suppress the drowsiness or pain reaction mediated by L-PGDS-catalyzed PGD₂ without showing the various side effects caused

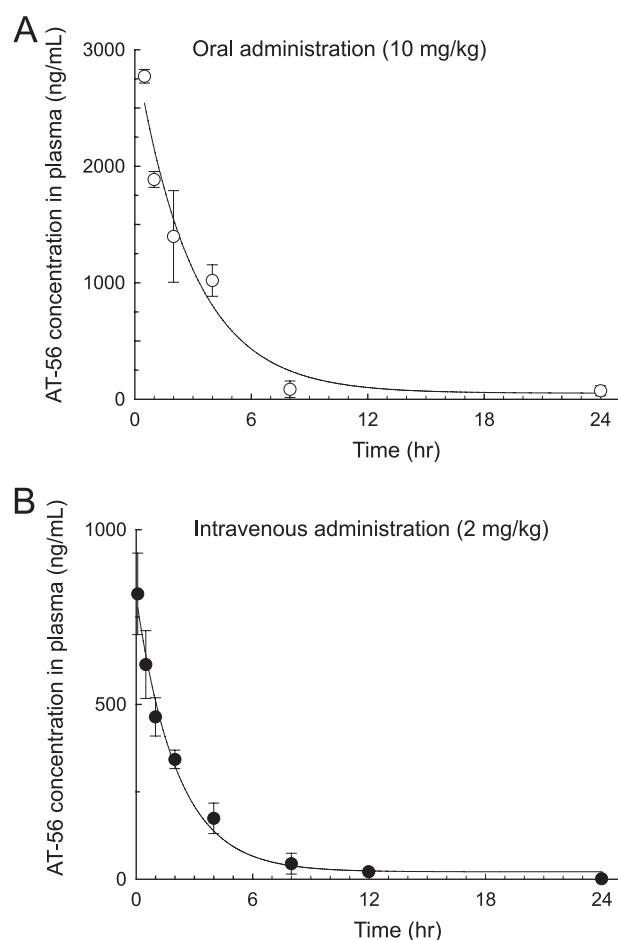


FIGURE 7. Time courses of plasma concentrations of AT-56 after oral (10 mg/kg) (A) or intravenous (2 mg/kg) (B) administration of AT-56 to C57BL/6 mice. Data are presented as the mean \pm S.E., $n = 3$ /time point.

TABLE 1
Pharmacokinetic parameters of AT-56

| Route | Dose | AUC ^a | C _{max} ^b | C ₀ ^c | t _{max} ^d | t _{1/2} ^e | BA ^f |
|---------------|-------|------------------|-------------------------------|-----------------------------|-------------------------------|-------------------------------|-----------------|
| | mg/kg | μg·h/ml | μg/ml | μg/ml | h | h | % |
| Intravenous | 2 | 1.28 | 0.86 | 0.08 | 2.35 | | |
| <i>Per os</i> | 10 | 8.95 | 2.15 | | 0.50 | 1.71 | 82.0 |

^a AUC, area under the concentration *versus* time curve from 0 to the last quantifiable time point.

^b C_{max}, maximal concentration.

^c C₀, initial concentration.

^d t_{max}, time to C_{max}.

^e t_{1/2}, half-life.

^f BA, bioavailability = (AUC *p.o.* × dose *i.v.*)/(AUC *i.v.* × dose *p.o.*) × 100, where *p.o.* represents *per os* and *i.v.* represents intravenous.

by the suppression of cytoprotective and anti-inflammatory PGs.

We did not detect any acute toxic effects of AT-56 after its oral administration even at a dose of 100 mg/kg. AT-56 possesses a direct and previously unknown inhibitory effect on L-PGDS *in vitro* and *in vivo*, suggesting that AT-56 might be a useful prototypic molecule to develop selective and/or nonselective inhibitors for L-PGDS and H-PGDS, which may act as anti-somnolence and anti-inflammatory drugs, respectively. The development of such selective and nonselective inhibitors of both enzymes would be helpful to determine the role of PGD₂ in animal models. Such inhibitors would be drug candidates or actual drugs.

Acknowledgments—We thank O. Hayaishi (Osaka Bioscience Institute) for generous support of this study. We also thank Dr. K. Shigeno and Dr. K. Tanaka (TAIHO Pharmaceutical Company) for chemical synthesis and pharmacokinetics analysis of AT-56, respectively; T. Tsurumura and M. Sakata (Osaka Bioscience Institute) for assistance in enzyme assays and in vivo experiments, respectively; and Dr. M. Mase (Nagoya City University Hospital) for providing human CSF.

REFERENCES

- Ueno, R., Ishikawa, Y., Nakayama, T., and Hayaishi, O. (1982) *Biochem. Biophys. Res. Commun.* **109**, 576–582
- Qu, W. M., Huang, Z. L., Xu, X. H., Aritake, K., Eguchi, N., Nambu, F., Narumiya, S., Urade, Y., and Hayaishi, O. (2006) *Proc. Natl. Acad. Sci. U. S. A.* **103**, 17949–17954
- Lewis, R. A., Soter, N. A., Diamond, P. T., Austen, K. F., Oates, J. A., and Roberts, L. J., 2nd. (1982) *J. Immunol.* **129**, 1627–1631
- Hirata, M., Kakizuka, A., Aizawa, M., Ushikubi, F., and Narumiya, S. (1994) *Proc. Natl. Acad. Sci. U. S. A.* **91**, 11192–11196
- Nagata, K., Hirai, H., Tanaka, K., Ogawa, K., Aso, T., Sugamura, K., Nakamura, M., and Takano, S. (1999) *FEBS Lett.* **459**, 195–199
- Mizoguchi, A., Eguchi, N., Kimura, K., Kiyohara, Y., Qu, W. M., Huang, Z. L., Mochizuki, T., Lazarus, M., Kobayashi, T., Kaneko, T., Narumiya, S., Urade, Y., and Hayaishi, O. (2001) *Proc. Natl. Acad. Sci. U. S. A.* **98**, 11674–11679
- Eguchi, N., Minami, T., Shirafuji, N., Kanaoka, Y., Tanaka, T., Nagata, A., Yoshida, N., Urade, Y., Ito, S., and Hayaishi, O. (1999) *Proc. Natl. Acad. Sci. U. S. A.* **96**, 726–730
- Matsuoka, T., Hirata, M., Tanaka, H., Takahashi, Y., Murata, T., Kabashima, K., Sugimoto, Y., Kobayashi, T., Ushikubi, F., Aze, Y., Eguchi, N., Urade, Y., Yoshida, N., Kimura, K., Mizoguchi, A., Honda, Y., Nagai, H., and Narumiya, S. (2000) *Science* **287**, 2013–2017
- Hirai, H., Tanaka, K., Yoshie, O., Ogawa, K., Kenmotsu, K., Takamori, Y., Ichimasa, M., Sugamura, K., Nakamura, M., Takano, S., and Nagata, K. (2001) *J. Exp. Med.* **193**, 255–261
- Urade, Y., Fujimoto, N., and Hayaishi, O. (1985) *J. Biol. Chem.* **260**, 12410–12415
- Urade, Y., Eguchi, N., and Hayaishi, O. (2006) in *Lipocalins* (Åkerström, B., Flower, D., and Salier, J.P., eds) Vol. 9, pp. 99–109, Landes Bioscience/Eurekah.com, Georgetown, TX
- Nagata, A., Suzuki, Y., Igarashi, M., Eguchi, N., Toh, H., Urade, Y., and Hayaishi, O. (1991) *Proc. Natl. Acad. Sci. U. S. A.* **88**, 4020–4024
- Urade, Y., and Hayaishi, O. (2000) *Biochim. Biophys. Acta* **1482**, 259–271
- Christ-Hazelhof, E., and Nugteren, D. H. (1979) *Biochim. Biophys. Acta* **572**, 43–51
- Urade, Y., Fujimoto, N., Ujihara, M., and Hayaishi, O. (1987) *J. Biol. Chem.* **262**, 3820–3825
- Urade, Y., Mohri, I., Aritake, K., Inoue, T., and Miyano, M. (2006) in *Functional and Structural Biology on the Lipo-network* (Morikawa, K. T., ed) pp. 135–164, Transworld Research Network, Karala, India
- Ujihara, M., Tsuchida, S., Satoh, K., Sato, K., and Urade, Y. (1988) *Arch. Biochem. Biophys.* **264**, 428–437
- Beuckmann, C. T., Lazarus, M., Gerashchenko, D., Mizoguchi, A., Nomura, S., Mohri, I., Uesugi, A., Kaneko, T., Mizuno, N., Hayaishi, O., and Urade, Y. (2000) *J. Comp. Neurol.* **428**, 62–78
- Beuckmann, C. T., Gordon, W. C., Kanaoka, Y., Eguchi, N., Marcheselli, V. L., Gerashchenko, D. Y., Urade, Y., Hayaishi, O., and Bazan, N. G. (1996) *J. Neurosci.* **16**, 6119–6124
- Eguchi, Y., Eguchi, N., Oda, H., Seiki, K., Kijima, Y., Matsu-ura, Y., Urade, Y., and Hayaishi, O. (1997) *Proc. Natl. Acad. Sci. U. S. A.* **94**, 14689–14694
- Gerena, R. L., Eguchi, N., Urade, Y., and Killian, G. J. (2000) *J. Androl.* **21**, 848–854
- Pinzar, E., Kanaoka, Y., Inui, T., Eguchi, N., Urade, Y., and Hayaishi, O. (2000) *Proc. Natl. Acad. Sci. U. S. A.* **97**, 4903–4907
- Malki, S., Nef, S., Notarnicola, C., Thevenet, L., Gasca, S., Mejean, C., Berta, P., Poulat, F., and Boizet-Bonhoure, B. (2005) *EMBO J.* **24**, 1798–1809
- Ragolia, L., Palaia, T., Hall, C. E., Maesaka, J. K., Eguchi, N., and Urade, Y. (2005) *J. Biol. Chem.* **280**, 29946–29955
- Tanaka, R., Miwa, Y., Mou, K., Tomikawa, M., Eguchi, N., Urade, Y., Takahashi-Yanaga, F., Morimoto, S., Wake, N., and Sasaguri, T. (2009) *Biochem. Biophys. Res. Commun.* **378**, 851–856
- Fujimori, K., Aritake, K., and Urade, Y. (2007) *J. Biol. Chem.* **282**, 18458–18466
- Hoffmann, A., Conrad, H. S., Gross, G., Nimtz, M., Lottspeich, F., and Wurster, U. (1993) *J. Neurochem.* **61**, 451–456
- Watanabe, K., Urade, Y., Mader, M., Murphy, C., and Hayaishi, O. (1994) *Biochem. Biophys. Res. Commun.* **203**, 1110–1116
- Gerena, R. L., Irikura, D., Urade, Y., Eguchi, N., Chapman, D. A., and Killian, G. J. (1998) *Biol. Reprod.* **58**, 826–833
- Tokugawa, Y., Kunishige, I., Kubota, Y., Shimoya, K., Nobunaga, T., Kimura, T., Saji, F., Murata, Y., Eguchi, N., Oda, H., Urade, Y., and Hayaishi, O. (1998) *Biol. Reprod.* **58**, 600–607
- Clausen, E., and Pedersen, J. (1961) *Ugeskr. Laeger.* **123**, 620–622
- Pervaiz, S., and Brew, K. (1987) *FASEB J.* **1**, 209–214
- Tanaka, T., Urade, Y., Kimura, H., Eguchi, N., Nishikawa, A., and Hayaishi, O. (1997) *J. Biol. Chem.* **272**, 15789–15795
- Beuckmann, C. T., Aoyagi, M., Okazaki, I., Hiroike, T., Toh, H., Hayaishi, O., and Urade, Y. (1999) *Biochemistry* **38**, 8006–8013
- Mohri, I., Taniike, M., Okazaki, I., Kagitani-Shimono, K., Aritake, K., Kanekiyo, T., Yagi, T., Takikita, S., Kim, H. S., Urade, Y., and Suzuki, K. (2006) *J. Neurochem.* **97**, 641–651
- Kanekiyo, T., Ban, T., Aritake, K., Huang, Z. L., Qu, W. M., Okazaki, I., Mohri, I., Murayama, S., Ozono, K., Taniike, M., Goto, Y., and Urade, Y. (2007) *Proc. Natl. Acad. Sci. U. S. A.* **104**, 6412–6417
- Kanaoka, Y., Ago, H., Inagaki, E., Nanayama, T., Miyano, M., Kikuno, R., Fujii, Y., Eguchi, N., Toh, H., Urade, Y., and Hayaishi, O. (1997) *Cell* **90**, 1085–1095
- Urade, Y., and Hayaishi, O. (2000) *Vitam. Horm.* **58**, 89–120
- Urade, Y., and Eguchi, N. (2002) *Prostaglandins Other Lipid Mediat.* **68**, 375–382
- Islam, F., Watanabe, Y., Morii, H., and Hayaishi, O. (1991) *Arch. Biochem. Biophys.* **289**, 161–166
- Matsumura, H., Takahata, R., and Hayaishi, O. (1991) *Proc. Natl. Acad. Sci. U. S. A.* **88**, 9046–9050
- Aritake, K., Kado, Y., Inoue, T., Miyano, M., and Urade, Y. (2006) *J. Biol. Chem.* **281**, 15277–15286
- Fujimori, K., Aritake, K., and Urade, Y. (2008) *Gene (Amst.)* **426**, 72–80
- Inui, T., Ohkubo, T., Emi, M., Irikura, D., Hayaishi, O., and Urade, Y. (2003) *J. Biol. Chem.* **278**, 2845–2852
- Irikura, D., Kumasaka, T., Yamamoto, M., Ago, H., Miyano, M., Kubata, K. B., Sakai, H., Hayaishi, O., and Urade, Y. (2003) *J. Biochem. (Tokyo)* **133**, 29–32
- Inoue, T., Irikura, D., Okazaki, N., Kinugasa, S., Matsumura, H., Uodome, N., Yamamoto, M., Kumasaka, T., Miyano, M., Kai, Y., and Urade, Y. (2003) *Nat. Struct. Biol.* **10**, 291–296
- Lazarus, M., Kubata, B. K., Eguchi, N., Fujitani, Y., Urade, Y., and Hayaishi, O. (2002) *Arch. Biochem. Biophys.* **397**, 336–341
- Yamamoto, S. (1982) *Methods Enzymol.* **86**, 55–60
- Shimamoto, S., Yoshida, T., Inui, T., Gohda, K., Kobayashi, Y., Fujimori, K., Tsurumura, T., Aritake, K., Urade, Y., and Ohkubo, T. (2007) *J. Biol. Chem.* **282**, 31373–31379
- Mahmud, I., Ueda, N., Yamaguchi, H., Yamashita, R., Yamamoto, S., Kanaoka, Y., Urade, Y., and Hayaishi, O. (1997) *J. Biol. Chem.* **272**, 28263–28266
- Trivedi, S. G., Newson, J., Rajakariar, R., Jacques, T. S., Hannon, R., Kanaoka, Y., Eguchi, N., Colville-Nash, P., and Gilroy, D. W. (2006) *Proc. Natl. Acad. Sci. U. S. A.* **103**, 5179–5184
- Fujitani, Y., Kanaoka, Y., Aritake, K., Uodome, N., Okazaki-Hatake, K., and Urade, Y. (2002) *J. Immunol.* **168**, 443–449
- Craik, D. J., and Wilce, J. A. (1997) *Methods Mol. Biol.* **60**, 195–232
- White, D. M., Takeda, T., DeGroot, L. J., Stefansson, K., and Arnason, B. G. (1997) *J. Biol. Chem.* **272**, 14387–14393